https://dx.doi.org/10.4314/ijs.v21i1.12

VISCO-ACOUSTIC DATA MODELING USING OPTIMUM LAYER APPROXIMATION TECHNIQUE: GREENWOOD OIL FIELD EXAMPLE, USA

Raji[1,2], W. O., Harris[1], J. M., Folorunsho[2], I. O. and Gao[1], Y
[1]Department of Geophysics, Stanford University, 397 Panama Mall, Stanford, CA 94305, USA
[2]Department of Geophysics, Faculty of Science, University of Ilorin, PMB 1515, Ilorin, Nigeria
Corresponding author's Email: wasiu.raji@gmail.com
(Received: 13th September, 2018; Accepted: 22nd January, 2019)

ABSTRACT

It is desirable to use Finite Element (FE) or Finite Difference (FD) method to simulate elastic data for cross-hole seismic surveys. But FE and FD are computationally intensive and time-expensive for full wave-field modeling of large cross-hole survey. The computation cost – space and time- of elastic data modeling inhibits the use of synthetic data for providing solution to cross-hole geophysics problems .On the other hand, acoustic synthetic data require less computation time but lacks some of seismic arrivals seen in the field data. In this study a recursive reflectivity method incorporating P and S wave properties and attenuation effects is formulated to model cross-hole seismic data. The model is tested using a set of field data acquired in Green Wood field, USA. The visco-acoustic data modeled by the recursive reflectivity method show improvement over the acoustic data and gave a perfect match to the elastic and field data. The visco-acoustic data featured the different seismic arrivals seen in the field and elastic synthetic data. The data simulation method is stable, efficient, and fast. The inclusion of a scheme for determining the optimum layer model further reduced the computation time without compromising the quality of the results: only about one-eight of the time require for elastic data is needed to produce the equivalent visco-acoustic data. Because of its low computation cost, the study highlights the strong potentials for solving the problem of inefficient algorithm for processing and imaging cross-hole data, with a consequence of using cross-hole technology as a routine in oil and gas industry.

Key words: Cross-hole seismic survey; synthetic data; acoustic wave simulation; visco-acoustic.

INTRODUCTION

With the recent development of numeric algorithm for modeling full and decomposed data for cross-hole seismic acquisitions, strong potential arose for better understanding of the different wave modes comprising cross-hole data. Synthetic modeling of seismic data has provided insights to field data thereby leading to improvements in data handling, signal processing, and reflection imaging of cross-hole data. Very often cross-hole field data are seen to be elastic. Therefore, cross-hole data are modeled using elastic wave simulation techniques (Harris et al., 1995; Lazaratos, 1995; Raji et al., 2017). However, elastic wave modeling for large cross-hole survey is computationally intensive and time-expensive. Given a incident wave on a layer below a half-space, an incident wave will give rise to more than 8 different wave arrival at the geophone position, namely: direct wave,P-waves, transmitted converted wave, up-going P-P reflection, down going P-Preflection, P-S reflections, S-wave direct arrival, S-S down-going reflection, S-S up-going reflection, S-P refraction among others. According to some numerical studies (Phadke and Ramanjulu, 2012; Raji et al., 2017) the computation time for elastic data is about 4 times higher than the time required to compute acoustic data of the same size. The computation time-difference becomes higher as the size of survey increases. For very large survey and complex geological model, the time difference between elastic and acoustic data can be up to days or weeks, whereas the difference in the features of the data is minimal (Zhou et al., 1995; Kosloof, 1989 et al., 1989; Phadke and Ramanjulu, 2012).

Acoustic data are seen to lack the complex wave modes that provide full account of the different seismic arrivals seen in cross-hole field data. Therefore, previous studies on cross-hole data modelling favoured elastic wave simulations. The arguments in some cross-hole geophysics papers (e.g., Muller, 1985; Meredith, 1990)are that some acoustic wave codes for cross-hole data simulation(i)are mere upgraded version of those used for surface seismic data modelling; (ii) the procedure failed to account for attenuation process caused by rocks anelasticity; (iii) and that the data, among other, failed to account for the

multidirectional arrivals from the layers above and below the sources and receivers. In reality, wave propagation through earth layers is best described by absorption models (Aki and Richard, 1980; Cerverny and Frangie, 1982) where the interaction between the waves and the pore fluids, and rock matrix contribute to energy loss in the propagating waves. Evolution of new techniques for modeling cross-hole acoustic synthetic data that will better-fit the field data is a requirement for reducing the computation time and computer space for handling cross-hole synthetic data. With this achievement, full data for large cross-hole seismic survey can be modeled in short time, thereby enabling on-the-field pre-survey data modeling to test different field geometry and predict potential problems in an on-gong seismic acquisition.

The renewed efforts in the study of crosswell geophysics data by synthetic modeling is to better understand: the behavior of waves between the sources' and receivers' wells; fluid flow at a scale that is unavailable in the conventional seismic data, well logs and core data. Understanding the reservoir pore structures at this unique scale is critical to optimizing primary production from reservoirs, choice of injection fluid, and optimal hydrocarbon recovery. On one hand, surface seismic profiling and generalized velocity modelling are often insufficient to illuminate reservoir-scale flow-discontinuity structures in deep-seated compartmentalized reservoirs (Leary et al. 2005). On the other hand, information from the core data and well logs has insufficient coverage to reflect the spatial attitude of large structures that could inhibit free flow of reservoir fluid. Cross-hole data has the resolution and coverage that are required to illuminate the small but important structures for optimum well citing and hydrocarbon production.

The advantages of cross-hole survey over surface seismic data are overwhelming (Hu et al., 1988; Khalil et al., 1991; Justice et al., 1993; Harris, 1995; Lee et al., 1995; Raji et al., 2016). But cross-hole seismology is not completely understood (Lazaratos et al., 1993; Long et al., 2001; Raji, 2016; Raji et al. 2017). Forward modeling using numerical but realistic geological properties is a reliable means to study the physical phenomena that occur at subsurface – beyond human eyes. This is the reason why synthetic modeling of cross-hole seismic data has been a topic of interest to cross-well geophysicists. The ultimate aim of this paper is to describe and apply an accurate and fast method of producing synthetic cross-hole seismic data that can be used to describe and study cross-hole field data. Fast and accurate modeling of seismic data for cross-hole field experiment is key to high-end solution to the problems of lack of standard procedure for processing cross-hole data and inappropriate algorithm for imaging cross-hole data. In this paper, cross-hole is used synonymously with cross-well.

MATERIAL AND METHOD

Description of the simulator

The simulation assumed that acoustic wave propagation in geological media can be described by 2D-acoustic wave equation. Given that the calculated seismogram, $\boldsymbol{\rho(x_r, t|x_s)_{cal}}$ at time t for a receiver at location $\boldsymbol{x_r(r = 1, 2, \ldots . N_s)}$ is:

$$\frac{1}{k(x_r)}\frac{\partial^2 \rho(x_r t|x_s)}{\partial t^2} - \nabla.\left[\frac{1}{\rho(x_r)}\nabla\boldsymbol{\rho(x_r, t|x_s}\right] = \boldsymbol{s(x_r\, t|x_s)}. \quad ..1$$

where $\boldsymbol{s(x_r, t|x_s)}$ is the source function, $k(x_r)$ is the bulk modulus, $\rho(x_r)$ is the density. The velocity is related to the bulk modulus as:

$$v(x) \quad \sqrt{k(x)//\rho(x)} \quad \ldots\ldots\ldots\ldots\ldots\ldots\ldots\ldots\ldots\ldots\ldots\ldots 2$$

Considering the effect of energy dissipation in partially saturated rocks – typical of hydrocarbon reservoirs, the velocity (v)of each geological layer can be described by a complex number as:

$$v_{(f)} = V(1 - i\alpha(w)/2\pi f) \quad \ldots\ldots\ldots\ldots\ldots\ldots\ldots\ldots\ldots\ldots\ldots\ldots 3$$

$$\alpha(w) = \pi f/Q(w)v(w) \quad \ldots\ldots\ldots\ldots\ldots\ldots\ldots\ldots\ldots\ldots\ldots\ldots 4$$

where α is the attenuation coefficient; f is the frequency; ω is the angular frequency; π is a constant (22/7) and Q is the rock quality factor. Each layer of the geological model is defined in terms of P-wave velocity, P-wave quality factor, S-wave velocity, S-wave quality factor, and density. The visco–acoustic simulator simulates wave propagation in the different layer using recursive

reflectivity approach (Muller, 1985; Raji et al., 2014).

Modeling of the acquisition parameters and the geological data

The field data to be modeled were acquired in greenwood oil field, U.S.A by an acquisition geometry that comprised 300 sources and 300 receivers deployed to source and receiver wells respectively. The source and receiver wells are separated by a nominal distance of 980 ft (300 m) ft. Sources are deployed into the source well at a regular interval of 5 ft. (1.5 m) between a depth level of 3000 and 5000 ft (~ 909 – 1515 m). Similarly, hydrophone receivers were deployed into the receivers well at 5 ft intervals between a depth level of 300 and 5000 ft. The field is named Greewood for the purpose of this paper because some proprietary information are disclosed. Because the data were acquired in the USA, the acquisition unit for distance is in feet (ft). Where necessary, standard unit equivalence is provided.

Data acquisition system used piezoelectric sources and hydrophone receivers. In the simulations, the behavior of a fluid-coupled piezoelectric source (Lee and Blanch 1984; Meredith, 1990) was modeled using axisymmetric radial point force. This creates a source radiation pattern that travelled in sub-vertical and lateral directions through the inter-well rock volume to the array of receivers in the receivers' well. The hydrophone receiver is modeled as the radiant stress component of the simulated wave-field following the method of Schoenberg (1986) and Van Schaak et al. (1995). The borehole fluid density is assumed to be 1.0 g/cm^3.Similar to the field parameters, we modeled 300 sources with a spacing of 1.5 m (~ 5 ft) and 300 hydrophone receivers with a spacing of 1.5m. The source energy is modeled as a Riecker wavelet with a peak frequency of 800 Hz.

The Geological data consisted of geological logs acquired from the source and receiver's wells. The three log suites important for the study are the density, P-wave sonic, and S-wave sonic logs. P-wave velocity and S-wave velocity logs were created from the respective sonic logs. For the elastic data modeling, the respective source and receiver well logs were interpolated over the inter-well space to create the geological model shown in Figure 1. For the acoustic data modeling, the well logs are blocked into layers using a layer-extraction algorithm based on relative changes in the log curve. Different layer numbers were extracted and tested for computing acoustic data. The full layer extraction reveals 3046 layers. Subsequently layers with similar properties were approximated to reduce the layers to numbers ranging from 3046 to 280 in order to save computation time. The blocked well logs for 554 layers at the source well are shown in Figure 2.

Modelling of seismic data

First, Elastic data were simulated for the full survey using the Finite Difference Method, the

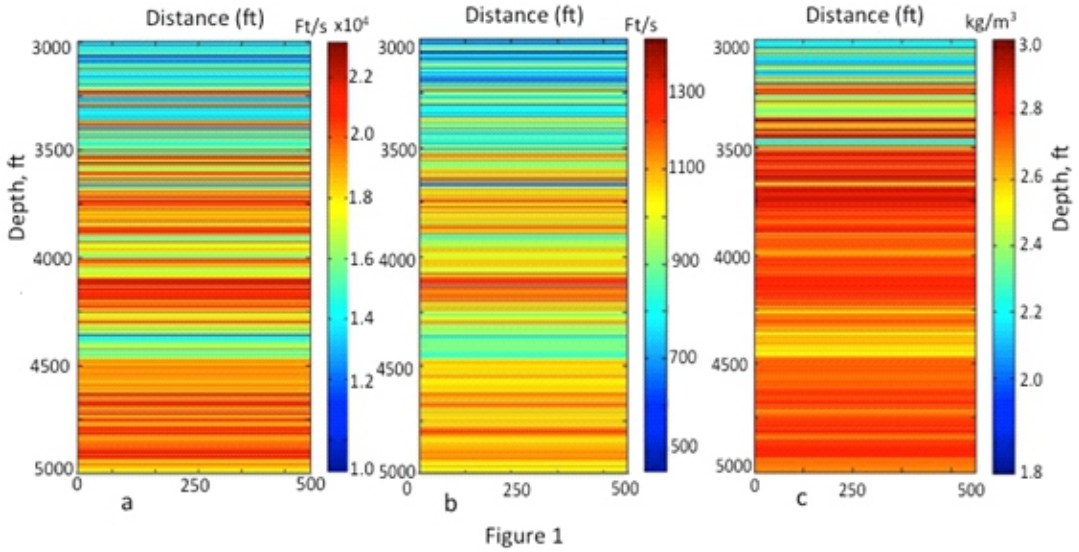

Figure 1: Geological Models. (a) P- wave velocity model, (b) S-wave velocity model, and (c) density models used to generate elastic (finite difference) synthetic data (Raji et al. 2017).

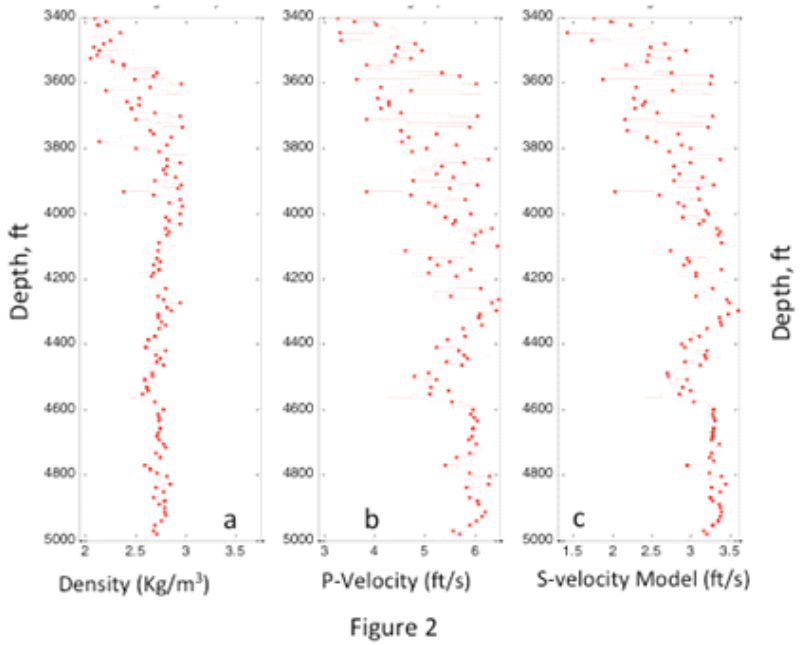

Figure 2: Blocked well logs for 544 Layers. (a) Density log, (b) P-wave velocity log, (c) S-wave Velocity log.

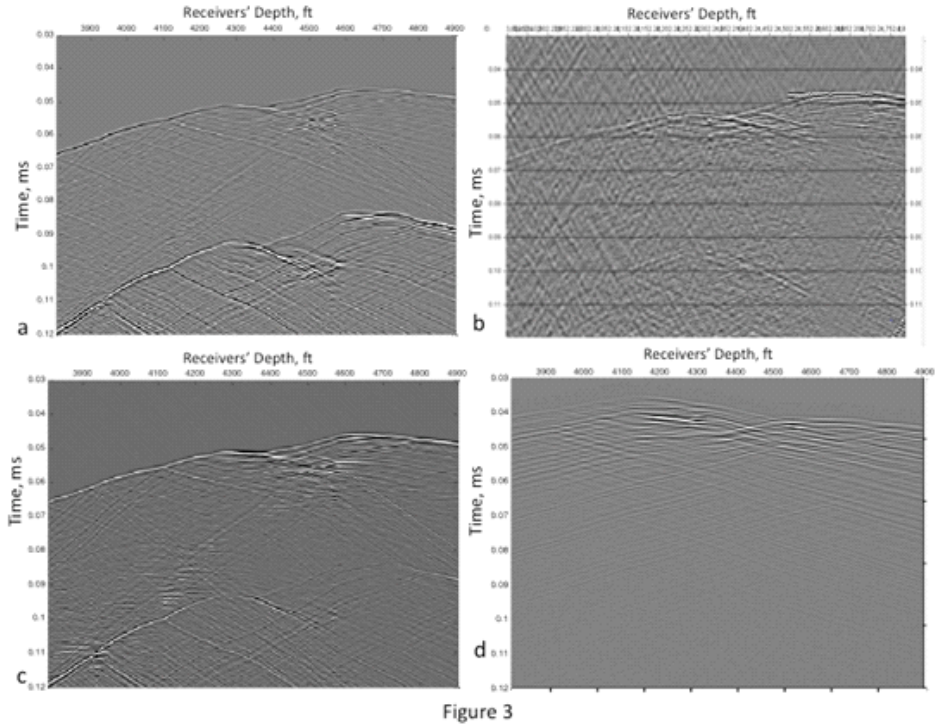

Figure 3: Comparing field data with different synthetic data: (a) visco-acoustic data; (b) field data; (c)elastic(finite difference) data, and (e) acoustic data.

geological model shown in Figure 1 and the survey described above. Procedure for the elastic data modelling using Finite Difference Methods are described in many geophysics papers (e.g., Hu et al., 1988; Bube and Langan, 2008; Zhu and Harris, 2015). Next, visco-acoustic data are simulated for the same survey using the visco-acoustic Simulator described above and 3046 geological layers model. The visco-acoustic, field, elastic, and acoustic data are compared in Figure 3. Subsequently, the visco-acoustic data is modeled using fewer numbers of layers. The layer numbers

tested with the model include 1056, 554, 228. For the different layer approximation models, the average slowness used in each block was chosen to match the total travel time calculated from the original log. This is to reduce the travel-time error in the calculated data. The Q value in the computation was 200.

DISCUSSION OF RESULTS

The visco-acoustic data (fig 3a) produced by the method described in this paper is consistent with the field data (Fig 3b) and elastic data (Fig 3c). Consistencies in these three data sets include a set of P-P reflections located at depths of (about) 3950 and 4100ft. The visco-acoustic data show superiority to the acoustic data (Fig3d) produced by the conventional acoustic wave equation. The result of this study shows that acoustic synthetic data can be used to study cross-hole field data if all the seismic wave modes are properly modeled. The improvement in the data in Figure 3a compared to that in figure 3d is due to the inclusion of the shear energy and the complex seismic wave modes in the recursive reflectivity algorithm (Muller, 1985) used for the visco-acoustic data simulation. The conventional method of modeling acoustic data follows the typical flow for modeling surface seismic data where shear wave properties are not usually considered. The simulation procedure for the visco-acoustic data shown in Figure 3a included shear (S) wave properties, incorporated energy loss due to attenuation, and used recursive reflectivity method to calculate energy from the different layers.

A comparison of the visco-acoustic data (Fig. 3a) with the elastic synthetic data (Fig. 3c) show that almost all the seismic arrivals in the elastic data are present in the visco-acoustic data, and the time required to produce the visco-acoustic data is about a quarter of the time needed to produce elastic data for the same survey. To further save computation time, the simulation included a routine to produce layered model from the logs and merged layers with similar acoustic parameters to obtain 1056, 554, 288 layers from the original 3046 layers. These layer models were used to produce the acoustic data shown in Figure 4b. It was observed from these results that the data produced with 1056, 554 layer models are compatible with the data produced using the full (3046) layer model, but data produced using 288-layer model is of lower quality. As seen in the visco-acoustic data produced by the model with 3046 layer, data in Figs. 4b and 4c contain sets of reflections including those from depths equivalence of 3950 and 4100 ft. These reflections are weak and a bit curvy in the data shown in Fig. 4d. In addition, the energy of the different seismic events in the data (produced from 288-layer model) are degraded. This could be due to merging of layers with significantly different acoustic properties (e.g., velocity). The purpose of presenting the result in Figure 4d is to show that despite the robustness of the simulation algorithm, the quality of the data produced partly depends on the quality of the geological model produced by blocking the well logs and hence the algorithm used for blocking the layer. The algorithm must be capable of recognizing subtle and distinct changes in acoustic parameters.

The result presented in Figure 4 among others (not shown in this paper) showed that 554 is about the optimum layer number for the model approximation test. Optimum layer number in this case is the least number of layers in the geological model that can produce data that best-fit the field data. Subsequently 554 layers model is used for our visco-acoustic modeling experiment. Comparison of computation time for elastic and visco-acoustic data was tested using common shot gather, CSG #181-190 showed that only about one-eight of the time required to produce elastic data is needed to produce the visco-acoustic data using 554 layers. Further to this, visco-acoustic data are produced for common shot gathers #267, #288, and #295 using 554 layers model and each gather is compared with the corresponding field data as shown in Figure 5. Again the comparison shows that the acoustic data is comparable to the field data. All the major seismic arrivals seen on the field data are present in the visco-acoustic synthetic data. Overall, there are striking similarities between the field and the visco-acoustic data for the corresponding gathers. The process of determining the optimum layer number is yet to be standardized. It is still based on educative-guess trial-by- error method.

Finally, the reverse time migration, RTM image of the full survey of visco-acoustic data and field data

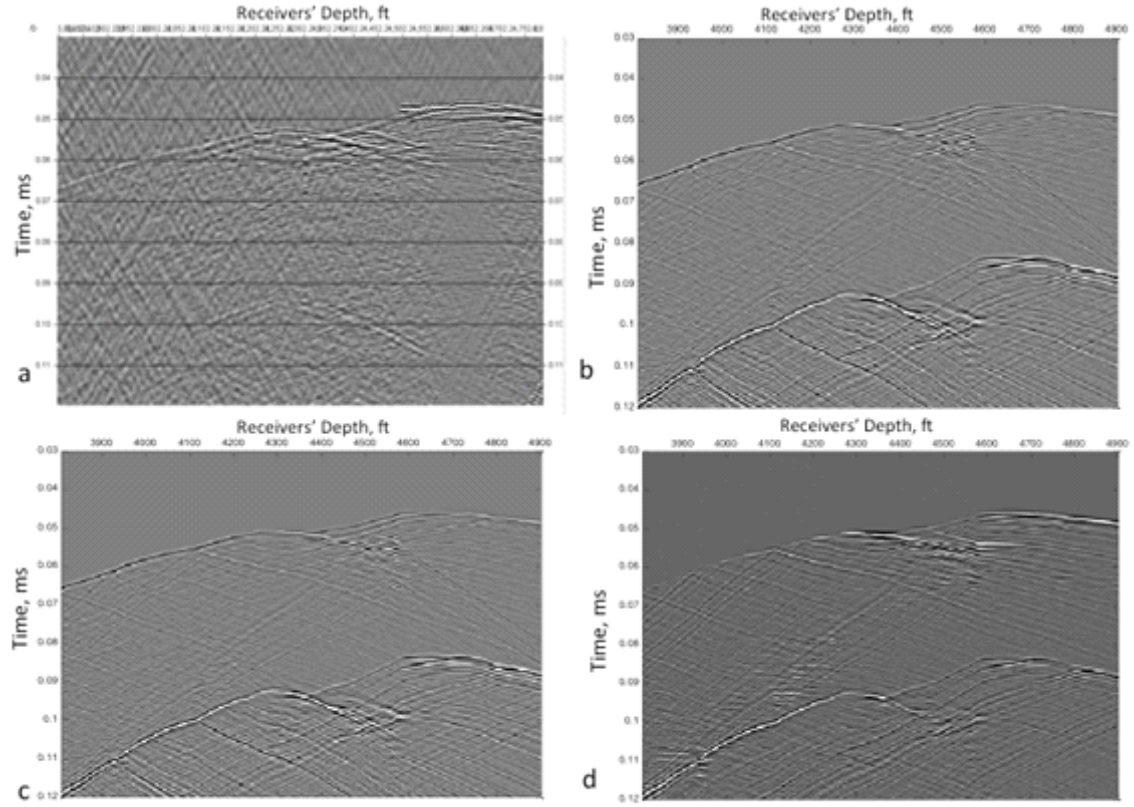

Figure 4

Figure 4: Field data versus visco-acoustic data using different layer models. (a) field data; (b) visco-acoustic data from 1056 layers model, (c) visco-acoustic data from 554 layers model, (d) visco-acoustic data from 280 layers model.

are produced as shown in Figure 6. The RTM used a smoothed version of the velocity tomogram built from the well logs. The velocity logs at the source and receiver wells are interpolated over the inter-well space. The interpolated velocity is tomographically inverted using ray-tracing method (Tikhonov and Arseni 1977; Langan et al., 1985; Nocedal and Wright, 1999; Zhu and Harris, 2015). The velocity model obtained after five iterations and the RTM results are shown in Figure 6. Prior to RTM imaging, the field data was minimally processed to remove energy bust, direct waves, low frequency events, and shear energies (Raji, 2016). The synthetic elastic data were processed only to remove direct arrival and the shear energy. The semblance in the RTM images of the field data (Fig. 6a) and visco-acoustic data (Fig. 6c) confirms the consistencies in the data and the appropriateness of method used in the study.

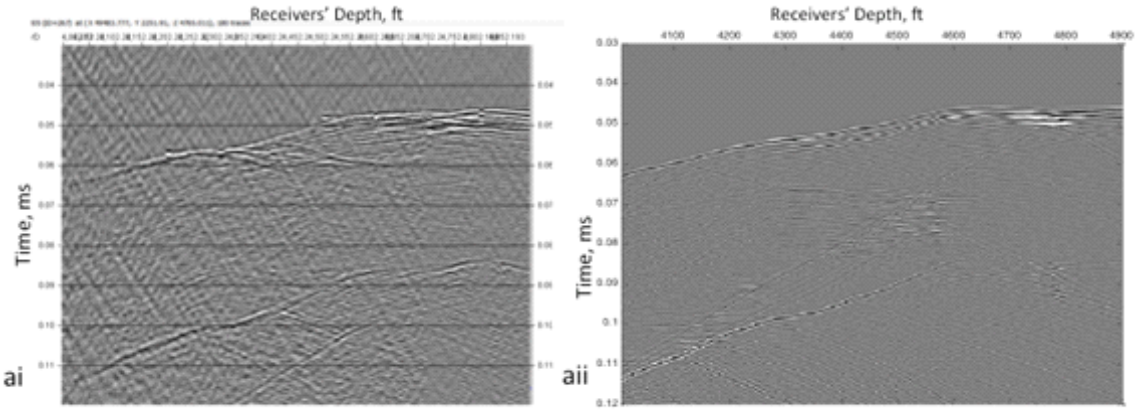

Figure 5a

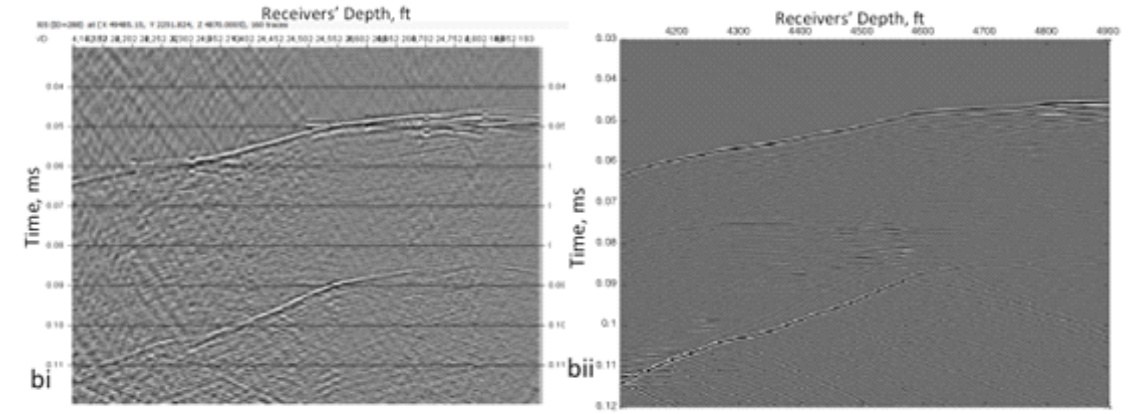

Figure 5b

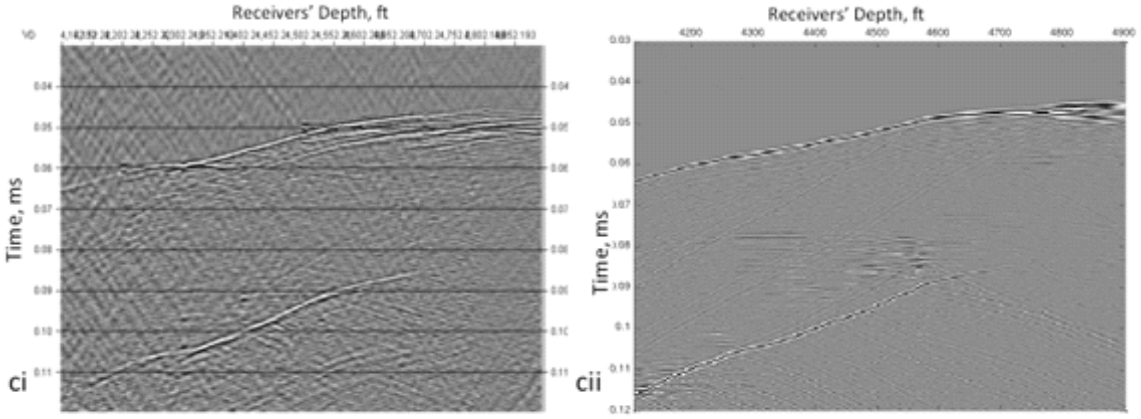

Figure 5c

Figure 5: Comparing field data with visco-acoustic data for different common source Gather, CSG. (a) Field data and acoustic data for CGS # 267, (b) Field data and acoustic data for CGS # 288, (c) Field data and acoustic data for CGS # 295.

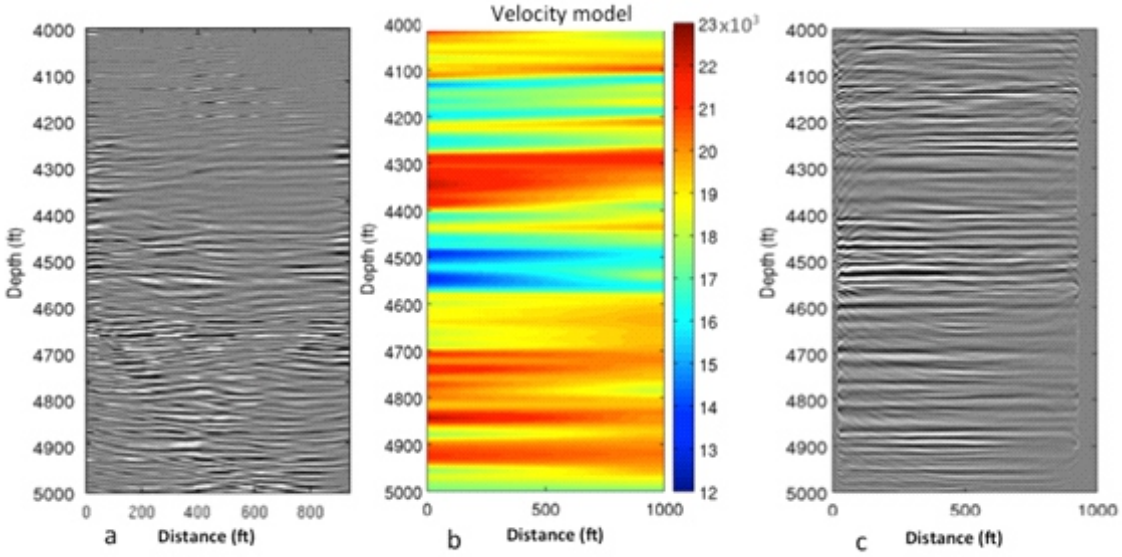

Figure 6

Figure 6: Reverse Time Migration (RTM) Results: (a) RTM of field data, (b) Velocity tomogram used for the RTM, (c) RTM of visco-acoustic data.

CONCLUSION

Visco-acoustic data produced for Green Wood Field cross-hole Seismic Survey provided robust evidence that visco-acoustic data modeled with the inclusion of shear energies, converted waves, and seismic attenuation effects can be used to approximate cross-hole field data. The acoustic wave simulation followed the recursive reflectivity procedure to calculate all the wave modes at the different geological layer. The acoustic data simulated by this method gave perfect match to the field data and the elastic data simulated by Finite Difference (FD) Method. The acoustic data modeling require only one-eight of the time needed to model FD elastic data. The data simulation scheme is accurate and stable for complex geological media. It has the potential, because of its time-inexpensiveness, to increase the utility of synthetic data for on-the-spot solution to cross-hole acquisition problems, and survey design. Synthetic data modeling as presented in this paper is the key to many high-end cross-well geophysics operations including: the design of standard procedure, which is currently lacking, for processing cross-hole data; development of cross-well imaging algorithm; and better understanding of the different wave modes present cross-well wave-field.

REFERENCES

Aki, K. and Richard, P. G. 1980. Quantitative seismology - theory and methods, W. F. Freeman and Company.

Bube, K., Langan, R., 2008. A continuation approach to regularization of ill-posed problems with application to crosswell-travel time tomography. Geophysics 73: 337–351.

Cerverny, V. and Frangie, A. B. 1982. Effect of causal absorption on seismic body wave. studia Geophysia geodaetica. springa Neitherland, 26: 238 -253.

Harris J. M., Nolen-Hoeksema R, Rector J.W., Lazaratos S.K. and Van Schaack M.A. 1995. High-resolution crosswell imaging of a west Texas carbonate reservoir: part I-project summary and interpretation. Geophysics 60:667–681

Hu, L, McMechan, G.A. and Harris J. M. 1988. Acoustic prestack migration of cross-hole data. Geophysics 53:1015–1023.

Justice, J.H., Mathisen, M.E., Vassiliou, A.A., Shiao, I., Alameddine, B.R. and Alhiliali, K.A. 1993. Crosshole seismic tomography in improved oil recovery. First Break 11: 229–239.

Khalil A.A., Stewart R.R and Henley D. C.1991. Full waveform processing and interpretation of kilohertz cross-well seismic data. Geophysics 58: 1248–1256

Kosloff, D., Filho A. Q., Tessmer, E., and Behle A. 1989. Numerical solution of the acoustic and elastic wave equations by a new rapid Expansion Method. Geophysical prospecting 37: 383-394.

Lazaratos S.K, Harris J.M. Rector J.W. and Van Schaack M. A. 1993. High resolution, cross-well reflection imaging: potential and technical difficulties. Geophysics 58:1270–1280

Lazaratos, S., Harris, J. M., Rector, J. W. and Van Schaack, M. 1995. High-resolution crosswell imaging of a west Texas carbonate reservoir: Part 4--Reflection imaging, Geophysics 60: 702-711.

Leary, P. C., Ayres, W., Yang, W. J. and Chang, X. F. 2005. Crosswell seismic waveguide phenomenology of reservoir sands and shales at offsets >600 m, Liaohe Oil Field, NE China. Geophysical Journal International 163 (1): 285–307.

Lee, D.O., Stevenson, V.M., Johnston, P.F. and Mullen, C.E., 1995. Time lapse seismic tomography to characterize flow structure in the reservoir during the thermal stimulation. Geophysics 60 (3): 660– 666.

Lee, M. and Balch, A. 1982, Theoretical seismic wave radiation from a fluid-filled borehole, Geophysics 47: 1308-1314.

Long, A. S., Hoffmann, H. J. and Du, B. 2001. Understanding elastic wavefield recording by detailed 3D survey planning and simulation. 15th annual conference of Australia Society of Exploration Geophysicists, Brisbane, Australia.

Meredith, J. A., 1990, Numeric and analytical modeling of downhole seismic sources: The near and far-field: Ph.D. thesis, Massachusetts Institute of Technology.

Muller, G. 1985. The reflectivity method: a tutorial. Journal of Geophysics 58: 153 - 174.

Nocedal, J.and Wright, S.J. 1999. Numerical Optimization. Springer, New York, USA.

Phadke, S. and Ramanjulu, M. 2012. 3D Acoustic and Elastic Wave Modeling on a High Performance Computing System. Search and Discovery Article #40899 Posted March 31, 2012.

Langan, R. T., Lerche, I. and Cutler, R. T. 1985. Tracing of rays through heterogeneous media: An accurate and efficient procedure. Geophysics 50(9): 1456-1465.

Raji, W. O., Olasehinde, P. I. Abubakar, H. O. Alabi, R. A. 2014. Inversion and Application of Seismic Q Factor: Field Dataset Examples. Pacific Journal of Science and Technology. 15(1): 318-327.

Raji, W. O. 2016. Reflections Enhancement Processing For Multi-Component Cross-Well Seismic Data. Journal of Mining and Geology 52(2), in Press

Raji, W. O., Gao, Y. and Harris, J. M. 2017. Wavefield analysis of crosswell seismic data. Arab J Geoscience 10:217, DOI 10.1007/s12517-017-2964-6

Raji W. O., Harris, J. M. and Lu, S. 2018. Seismic velocity tomography for CO2 monitor in subsurface geological structures. Journal of King Saud University – Science. 30, 57-64.

Schoenberg, M. 1986, Fluid and solid motion in the neighborhood of a fluid-filled borehole due to the passage of a low-frequency elastic plane wave, Geophysics 51, 1191-1205.

Tikhonov, A.N. and Arsenin, V.Y. 1977. Solutions of Ill-posed Problems. W. H. Winston and Sons.

Van Schaack, M., Harris, J. M., Rector, J. W. and Lazaratos, S., 1995, High-resolution crosswell imaging of a west Texas carbonate reservoir: Part 2-Wavefield modeling and analysis, Geophysics 60, 682—691.

Zhou, C, Cai, W., Luo, Y. Schuster, G. T. and Hassanzadehs, S. 1995. Acoustic wave-equation travel time and waveform inversion of crosshole seismic data. Geophysics 60(3): 765-773.

Zhu, T., and Harris, J.M., 2015. Application of boundary-preserving seismic tomography for delineating boundaries of reservoir and CO2 saturated zone. Geophysics 80 (2): M33–M41. http://dx.doi.org/10.1190/geo2014-0361.1.